

---

MASTER'S THESIS

Specialty

**Fundamental Mathematics**

Grenoble Alpes University, Fourier Institute (Grenoble)

---

Presented by

**Paul COTTALORDA**

To obtain a

**MASTER'S DEGREE from GRENOBLE ALPES  
UNIVERSITY**

Master's thesis subject :

**Intersection norms over the homology groups of surfaces**

defended on June the 10<sup>th</sup> 2016

before a jury composed of :

Pr. François DAHMANI

Pr. Stéphane GUILLERMOU

Pr. Damien GAYET



## Introduction

This master thesis is the product of the work done during the internship of my Master 2 in Fundamental Mathematics under the supervision of Dr. Pierre Dehornoy. The subject belongs to the field of low-dimensional topology, and more precisely to the study of intersection of curves on surfaces. The internship mostly consisted in studying a recent family of norms that are similar to the Thurston norm, but for 2-manifolds and with a multi-curve as a parameter, called intersection norms.

Let us explain quickly intersection norms: for  $\Sigma$  a compact surface and  $\gamma$  a finite collection of curves on  $\Sigma$ , the norm  $x_\gamma$  is defined on  $H_1(\Sigma; \mathbb{Z})$  by minimizing, for curves in the considered class, the number of intersection points with  $\gamma$ . It extends uniquely to a semi-norm on  $H_1(\Sigma; \mathbb{R})$ .

My work was twofold. On the one hand, I studied general properties of such norms and especially focused on the case of the torus which is the simplest one. On the other hand, I developed a program that allows to compute examples of intersection norms.

The first section of this report introduces particular norms called integral norms (that include intersection norms) and studies some of their properties. The intersection norms are then introduced in the second section and we give combinatorial tools to study them. In the third section, we focus our study on the particular case of the torus and prove the main theorem of this master. The latter stipulates that any integral norm on the plane can be realized by a collection of geodesics on the torus and we explicit such a collection. The fourth and last section of this master thesis is dedicated to present the program I developed during this internship and give a quick guide on how to use it.

I would also like to take some few lines to thank my tutor Dr. Dehornoy for his patience and his availability all along this internship and for having always been there to answer my interrogations.



# Contents

<b>1</b>	<b>Integral norms over <math>\mathbb{R}^n</math></b>	<b>7</b>
1.1	Definition . . . . .	7
1.2	Properties . . . . .	7
1.2.1	Characterization of the unit ball of integral norms . . . . .	7
1.2.2	Decomposition theorem . . . . .	8
<b>2</b>	<b>Intersection norms</b>	<b>9</b>
2.1	Intersection number . . . . .	9
2.1.1	Definitions . . . . .	9
2.1.2	General properties . . . . .	10
2.2	Intersection norms . . . . .	11
2.2.1	Extension over $H_1(\Sigma, \partial\Sigma; \mathbb{R})$ . . . . .	11
2.3	Intersection norms and Eulerian coorientations . . . . .	12
<b>3</b>	<b>Intersection norms on the flat torus</b>	<b>13</b>
3.1	Normal polygons and Minkowski sum . . . . .	13
3.1.1	Definitions . . . . .	13
3.2	Case of geodesics on the flat torus . . . . .	15
3.2.1	Geodesics and minimality . . . . .	15
3.2.2	Intersection norms of family of geodesic . . . . .	16
3.2.3	Intersection norm and dual unitary ball of the intersection norm of a geodesic . . . . .	17
3.2.4	Fulness theorem on the torus . . . . .	17
<b>4</b>	<b>Software</b>	<b>18</b>
4.1	Presentation . . . . .	18
4.1.1	Limitations . . . . .	18
4.1.2	Features . . . . .	18
4.2	Quick guide . . . . .	19
4.2.1	Choosing the genus . . . . .	20
4.2.2	Entering the closed multi-curves . . . . .	20
4.3	Performances . . . . .	24
4.4	Possible improvement . . . . .	26

## List of Figures

1	The chain of circle is composed of null homotopic curves but there always be at least two intersections with any curves homotopic with the red one. .	10
2	Illustration of Theorems 21. On the left a collection $\gamma$ of four geodesics on the torus $\mathbb{T}^2$ , and a Eulerian coorientation (blue arrows). On the right the dual unit ball $B_\gamma^* \subset H_1(\mathbb{T}^2; \mathbb{Z})$ of the associated intersection norm. The empty circle denotes the origin. The big dots denote those classes in $H_1(\mathbb{T}^2; \mathbb{Z})$ congruent to $[\gamma]_2 \bmod 2$ . . . . .	12
3	Illustration of Definition 25: On the right we see the convex polygon composed of the family of vectors on the left . . . . .	13
4	Illustration of the contraction of the face that supports the transparent red band of the normal polygon. From left to right, one can see the polygon before and after the contraction . . . . .	14
5	The software at runtime. One can see from the background to the foreground Microsoft Visual Studio, and the console user interface and the control window . . . . .	18
6	Screenshot of the output of one execution of the program . . . . .	19
7	The control Window . . . . .	19
8	$\LaTeX$ file generated by the software . . . . .	19
9	The program at runtime: Opening of the control window. . . . .	20
10	The program at runtime: Beginning to set the polylines. . . . .	21
11	The program at runtime, with the cursor on the boundary. . . . .	22
12	The program at runtime: Setting of multiple curves. . . . .	22
13	The program at runtime: Output of the program. . . . .	23
14	File generated by the program. . . . .	23

# 1 Integral norms over $\mathbb{R}^n$

## 1.1 Definition

**Definition 1.** A norm  $\mu : \mathbb{R}^n \rightarrow \mathbb{R}$  is said to be integral if and only if it takes integral values on the integral lattice, i.e., for every  $x \in \mathbb{Z}^n$  we have  $\mu(x) \in \mathbb{Z}$ .

The general study of such norms is interesting because they appear when studying Thurston norms or intersection norms, those two being integral norms by definition. The following section is dedicated to proving a fundamental result (Theorem 6) due to William Thurston [Thu86] in the article defining the Thurston norm. Thurston gave a proof in dimensions 2 and 3, and declares that an induction works in higher dimensions.

## 1.2 Properties

### 1.2.1 Characterization of the unit ball of integral norms

The first three lemmas of this section are introduced to simplify the main result. They respectively give information on the asymptotic evolution of the intersection norm over "offset rays" (Lemma 2), on the local evolution of the intersection norm over "offset rays" (Lemma 3 and Corollary 4) and a sufficient condition for a simplex to be a part of the unit sphere of a norm (Lemma 5)). In this section,  $\mu$  denotes an arbitrary integral norm.

**Lemma 2.** For every  $a_0, b_0 \in (\mathbb{R}^n)^*$  we have  $\mu(a_0 + nb_0) \sim n\mu(b_0)$

*Proof.* By convexity of  $\mu$ , we have  $-\mu(-a_0) + n\mu(b_0) \leq \mu(a_0 + nb_0) \leq \mu(a_0) + n\mu(b_0)$ .  $\square$

**Lemma 3.** For every  $a_0, b_0 \in (\mathbb{Z}^n)^*$  the sequence  $\Delta : n \rightarrow \mu(a_0 + (n+1)b_0) - \mu(a_0 + nb_0)$  is increasing.

*Proof.* We have  $\Delta_{n+1} - \Delta_n = (\mu(a_0 + (n+2)b_0) - \mu(a_0 + (n+1)b_0)) - (\mu(a_0 + (n+1)b_0) - \mu(a_0 + nb_0))$ . By rearranging the terms we then have  $\Delta_{n+1} - \Delta_n = \mu(a_0 + (n+2)b_0) + \mu(a_0 + nb_0) - \mu(2a_0 + 2(n+1)b_0)$ . The latter is positive by convexity of  $\mu$ .  $\square$

**Corollary 4.** For every  $a_0, b_0 \in (\mathbb{Z}^n)^*$ , there exists  $n_0 \in \mathbb{N}$  such that for all  $n \geq n_0$  we have  $\mu(a_0 + nb_0) = \mu(a_0 + n_0b_0) + (n - n_0)\mu(b_0)$ .

*Proof.* The sequence  $\Delta$  from Lemma 3 is  $\mathbb{Z}$ -valued, increasing and bounded by  $\mu(b_0)$ , hence there exists a rank  $n_0$  and an integer  $\delta$  such that for all  $n \geq n_0$ ,  $\Delta_n = \delta$ . From Lemma 2, we have  $\delta = \mu(b_0)$  which proves the corollary.  $\square$

**Lemma 5.** Let  $\mu : \mathbb{R}^n \rightarrow \mathbb{R}$  be a norm on  $\mathbb{R}^n$ ,  $n > 1$ . Let  $\sigma = [x_1, \dots, x_n]$  be a  $(n-1)$ -simplex in  $\mathbb{R}^n$  such that for all  $i \in [1; n]$ ,  $\mu(x_i) = 1$ . If for some  $\bar{x} \in \overset{\circ}{\sigma}$  we have  $\mu(\bar{x}) = 1$ , then the restriction of  $\mu$  over  $\sigma$  is constant and equal to 1.

*Proof.* Consider  $x$  a point in  $\sigma = [x_1, \dots, x_n]$ . Since  $\mu$  is sub-additive, we have  $\mu(x) \leq 1$ . There exists a set of indices  $I$  with  $|I| = n-1$  such that  $\bar{x} \in \langle x, (x_i)_{i \in I} \rangle$ . We rewrite this family as  $J = (x'_1, \dots, x'_n)$ , and denote by  $(\lambda_1, \dots, \lambda_n)$  the barycentric coordinate of  $\bar{x}$

with respect to  $J$ . We have  $1 = \mu(\bar{x}) = \mu\left(\sum_{i=1}^n \lambda_i x'_i\right) \leq \sum_{i=1}^n \lambda_i \mu(x'_i) = \lambda_1 \mu(x) + (1 - \lambda_1)$ .

Hence we either have  $\mu(x) = 1$  or  $\lambda_1 = 0$ . Since  $\bar{x}$  is not contained in any face of  $\sigma$  we have  $\lambda_1 \neq 0$  and therefore  $\mu(x) = 1$ .  $\square$

The next theorem is due to Thurston [Thu86]. Thurston's proof is a bit heavy, and he only wrote it explicitly in dimension 3. We provide an alternative proof that is easier to write in every dimension.

**Theorem 6** (Characteristic of the unit ball of integral norms). *Assume that  $\mu$  is an integral norm. Then the unit sphere  $\partial B_\mu$  is composed of finitely many faces given by linear 1-forms with integral coefficients.*

*Proof.* Let  $(e_1, \dots, e_n)$  be a basis of  $\mathbb{Z}^n$  contained in the strict upper half space. We set for all  $n \in \mathbb{N}$   $a_n^1 = e_1 + ne_2$ . Thanks to Lemma 4 there exists a rank  $n_2$  such that for all  $n \geq n_2$  we have  $\mu(a_n^1) = \mu(a_{n_2}^1) + (n - n_2)\mu(e_2)$ . Furthermore,  $\mu(a_{n_2+1}^1) = \mu(a_{n_2}^1) + \mu(e_2)$ .

We then have

$$\frac{a_{n_2+1}^1}{\mu(a_{n_2+1}^1)} = \frac{a_{n_2}^1 + e_2}{\mu(a_{n_2}^1) + \mu(e_2)} = \frac{\mu(a_{n_2}^1)}{\mu(a_{n_2}^1) + \mu(e_2)} \frac{a_{n_2}^1}{\mu(a_{n_2}^1)} + \frac{\mu(e_2)}{\mu(a_{n_2}^1) + \mu(e_2)} \frac{e_2}{\mu(e_2)}$$

So  $\overline{a_{n_2+1}^1}$  belongs to  $\overset{\circ}{\left[ a_{n_2}^1, \overline{e_2} \right]}$ , hence  $\mu$  is constant and equal to 1 over the simplex  $\sigma_2 = \left[ \overline{a_{n_2}^1}, \overline{e_2} \right]$ .

Using the same process, we construct recursively a simplex  $\sigma_i$ ,  $i \geq 3$  by considering the sequence  $a_n^i = a_{n_{i-1}+1}^{i-1} + ne_i$ ,  $n_{i-1}$  being defined similarly to  $n_2$ . The dimension of  $\sigma_i$  increases by 1 at each step since  $(e_1, \dots, e_n)$  is a basis. The construction of the simplex ensures that, for all  $i$ , the restriction of  $\mu$  over  $\sigma_i$  is equal to 1, hence the  $(n-1)$ -simplex  $\sigma_n$  is a part of  $\partial B_\mu$ . Hence over the cone supported by  $\sigma_n$  in  $\mathbb{S}^n$  (we remind that since all  $e_i$  are contained in a half space, by construction,  $\sigma_n$  also is),  $\mu$  coincide with a 1-form with integral coefficients. By a change of basis, we can deduce that  $\partial B_\mu$  is composed of simplices given by 1-forms with integral coefficients. Since there exists a ball with diameter  $r > 0$  centered at 0 strictly contained in  $B_\mu$ , there exists finitely many 1-forms with integral coefficients that determine a face in  $\partial B_\mu$  (since there exists finitely many norms that do not intersect  $B_{\|\cdot\|_2}(r, 0)$ ) and therefore,  $\partial B_\mu$  is composed of finitely many simplices so  $\partial B_\mu$  is polyhedral.  $\square$

Equivalently, this means that the closed unit ball of the dual norm on  $(\mathbb{R}^n)^* \simeq \mathbb{R}^n$  is the convex hull of finitely many integer points.

Another proof of this theorem that relies on a dual approach is due to Mikaël de la Salle [Sal16].

**Corollary 7.** *Let  $\mu$  be an integral norm. Then the unit dual sphere  $\partial B_\mu^*$  is polyhedral (eventually degenerated) and the vertex belongs to the integral lattice.*

### 1.2.2 Decomposition theorem

Concerning intersection norms, a natural question is: considering two closed multi-curves  $\gamma_1$  and  $\gamma_2$ , can one compute the unit ball  $B_{\gamma_1 \cup \gamma_2}$  using only  $B_{\gamma_1}$  and  $B_{\gamma_2}$ . We will see that there exists an easy way to express  $B_{\gamma_1 \cup \gamma_2}^*$  as a function of  $B_{\gamma_1}^*$  and  $B_{\gamma_2}^*$  if the norm is additive with regards to the union *i.e.*  $\mu_{\gamma_1 \cup \gamma_2} = \mu_{\gamma_1} + \mu_{\gamma_2}$ . Denote by  $\oplus$  the Minkowski sum (Definition 24). This is actually a consequence of a more generic theorem that does not involve intersection norms and that we prove here:

**Proposition 8.** *Let  $\mu_1$  and  $\mu_2$  be two semi-norms over  $\mathbb{R}^n$ . Then for the unit balls of the dual norms we have*

$$B_{\mu_1 + \mu_2}^* = B_{\mu_1}^* \oplus B_{\mu_2}^*.$$



*Proof.* Since the case where one of the semi-norms is null is trivial, we only consider the case where both  $\mu_1$  and  $\mu_2$  are non-null.

We first prove the right inclusion  $B_{\mu_1+\mu_2}^* \subseteq B_{\mu_1}^* \oplus B_{\mu_2}^*$ . Consider  $\varphi \in B_{\mu_1+\mu_2}^* \subseteq H_1(\Sigma, \partial\Sigma; \mathbb{R})^* = \mathbb{R}^n$ . By definition we have  $(\mu_1 + \mu_2)^*(\varphi) \leq 1$ . By hypothesis, we then have  $\mu_1^*(\varphi) + \mu_2^*(\varphi) \leq 1$ . We directly deduce that  $\mu_{\gamma_1}^*(\varphi) \leq 1$  and  $\mu_{\gamma_2}^*(\varphi) \leq 1$ . Which leads to the first inclusion:  $B_{\mu_1+\mu_2}^* \subseteq B_{\mu_1}^* \oplus B_{\mu_2}^*$ .

Now we prove the converse inclusion. Recall that by definition we have

$$B_{\mu_1}^* \oplus B_{\mu_2}^* = \{ \varphi + \psi \mid \varphi \in B_{\mu_1}^*, \psi \in B_{\mu_2}^* \}.$$

Consider  $\varphi \in B_{\mu_1}^*$ ,  $\psi \in B_{\mu_2}^*$ . Then we have

$$(\mu_1 + \mu_2)^*(\varphi + \psi) = \sup_{(\mu_1+\mu_2)(x) \leq 1} |(\varphi + \psi)(x)| = \sup_{\mu_1(x)+\mu_2(x) \leq 1} |(\varphi + \psi)(x)|.$$

Hence there exists a sequence  $(x_n)_{n \in \mathbb{N}} \in (B_{\mu_1+\mu_2})^{\mathbb{N}}$  such that  $\lim_{n \rightarrow +\infty} |(\varphi + \psi)(x_n)| = (\mu_1 + \mu_2)^*(\varphi + \psi)$ . We can choose  $(x_n)_{n \in \mathbb{N}}$  such that for all  $n \in \mathbb{N}$ ,  $\mu_1(x_n) \neq 0$  and  $\mu_2(x_n) \neq 0$ . We then have

$$\varphi(x_n) + \psi(x_n) = \mu_1(x_n)\varphi\left(\frac{x_n}{\mu_1(x_n)}\right) + \mu_2(x_n)\psi\left(\frac{x_n}{\mu_2(x_n)}\right).$$

Since  $\varphi \in B_{\mu_1}^*$  and  $\psi \in B_{\mu_2}^*$ , we have  $\varphi\left(\frac{x_n}{\mu_1(x_n)}\right) \leq 1$  and  $\psi\left(\frac{x_n}{\mu_2(x_n)}\right) \leq 1$  which leads to

$$\varphi(x_n) + \psi(x_n) \leq \mu_1(x_n) + \mu_2(x_n) \leq 1.$$

By taking the limit, we have  $(\mu_1 + \mu_2)^*(\varphi + \psi) \leq 1$ , hence  $\varphi + \psi \in B_{\mu_1+\mu_2}^*$  which completes the proof for the second inclusion, and therefore completes the proof of the theorem.  $\square$

We will apply Proposition 8 to intersection norms in the some case where one can check that the norm is additive with respect to the union of curves, as we will see is the case of geodesic collections on the torus.

## 2 Intersection norms

### 2.1 Intersection number

#### 2.1.1 Definitions

**Definition 9.** Let  $\Sigma$  be a real compact surface with or without boundaries. A curve on  $\Sigma$  is the image of an immersion of the circle  $\mathbb{S}^1$  into  $\Sigma$  which is ambient isotopic to a poly line on  $\Sigma$ .

**Definition 10.** Let  $\Sigma$  be a real compact surface with or without boundaries. A closed multi-curve (or multi-curve for short) on  $\Sigma$  is a finite collection of closed curves in general position, that is, such that the curves are transversal with respect to themselves and to each other.

**Definition 11.** Let  $\gamma$  denote a fixed multi-curve on a compact surface  $\Sigma$ . For  $\alpha$  another multi-curve on  $\Sigma$ , the geometric intersection  $i_\gamma(\alpha)$  is the minimal number of intersections between  $\gamma$  and a multi-curve  $\rho$  homotopic to  $\alpha$ .

**Remark 12.** Beware that this definition is not symmetric since  $\gamma$  is fixed and not allowed to change in its homotopy class.

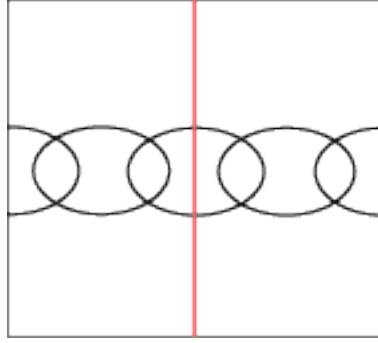


Figure 1: The chain of circle is composed of null homotopic curves but there always be at least two intersections with any curves homotopic with the red one.

Given a closed multi-curve  $\gamma$  this definition induces a function  $x_\gamma : H_1(\Sigma, \partial\Sigma; \mathbb{Z}) \rightarrow \mathbb{N}$  defined by

$$x_\gamma(a) := \min_{[\alpha]=a} i_\gamma(\alpha)$$

Since the number of intersections is always an integer number,  $x_\gamma$  is effectively defined by a minimum, the lower bound being always realized by a closed multi-curve.

**Definition 13.** Consider  $\gamma$  a closed multi-curve on  $\Sigma$ . A multi-curve  $\alpha$  is said to be minimizing (or minimal) with respect to  $x_\gamma$  if and only if,

$$i_\gamma(\alpha) = x_\gamma(\alpha).$$

If there is no ambiguity, we will just say that a closed multi-curve  $\alpha$  is minimizing.

**Lemma 14** (Geometric simplification). For any closed multi-curve  $\gamma$  and any homotopy class  $a$  in  $H_1(\Sigma, \partial\Sigma; \mathbb{Z})$ , there exist a simple curve  $\alpha$  such that  $[\alpha] = a$  and  $x_\gamma(a) = i_\gamma(\alpha)$ .

### 2.1.2 General properties

**Lemma 15** (Linearity).  $x_\gamma$  is linear over the rays i.e.

$$\forall a \in H_1(\Sigma, \partial\Sigma; \mathbb{Z}), \forall n \in \mathbb{N}, x_\gamma(n.a) = n.x_\gamma(a)$$

*Proof.* The inequality  $x_\gamma(n.a) \leq n.x_\gamma(a)$  is immediate since a closed multi-curve composed of  $n$  parallel copies of  $\alpha$  have an intersection number  $i_\gamma(n.a) = n.i_\gamma(a)$ . Reciprocally, if we consider a minimizing closed multi-curve  $\alpha$  in the homotopy class  $a$ . Lemma 14 allows us to choose a simple one. Since  $[\alpha]$  is a class divisible by  $n$ , the class of  $\alpha$  is null in  $H_1(\Sigma, \partial\Sigma; \mathbb{Z}/n\mathbb{Z})$ . This implies that the connected regions of  $\Gamma \setminus \alpha$  can be labeled from  $0, \dots, n-1 \pmod n$ , such that the label increase when we go from one region to another by crossing  $\alpha$  positively. The closed multi-curve  $\alpha$  can then be seen as the reunion of  $n$  close multi-curves: the ones that separate the region 0 from the region 1, the region 1 from the region 2, and so on. Each of these closed multi-curves has  $a$  as homology class. If one of these was not minimal, we could replace it by a minimal one, which would be incompatible with  $\alpha$  being minimal. Hence, each one of these closed multi-curves cross  $\gamma$   $x_\gamma(a)$  times and therefore  $x_\gamma(n.a) = n.x_\gamma(a)$ .  $\square$

**Lemma 16** (Triangular inequality).  $x_\gamma$  is subadditive, i.e.

$$\forall (a, b) \in H_1(\Sigma, \partial\Sigma; \mathbb{Z}), x_\gamma(a + b) \leq x_\gamma(a) + x_\gamma(b)$$

*Proof.* The union of two closed multi-curves realizing  $x_\gamma(a)$  and  $x_\gamma(b)$  intersect  $\gamma$   $x_\gamma(a) + x_\gamma(b)$  times.  $\square$

**Lemma 17.** *For all  $a$  in  $H_1(\Sigma, \partial\Sigma; \mathbb{Z})$ ,  $x_\gamma(a) = x_\gamma(-a)$ .*

*Proof.* The intersection number is a geometric definition and does not depend on the orientation of the closed multi-curve.  $\square$

**Corollary 18.** *The intersection number  $x_\gamma$  of a curve is the absolute value of a  $\mathbb{Z}$ -linear function i.e.*

$$\forall a \in H_1(\Sigma, \partial\Sigma; \mathbb{Z}), \forall n \in \mathbb{Z}, x_\gamma(n.a) = |n.x_\gamma(a)|$$

The property of  $x_\gamma$  reminds us of semi-norms and in fact we are going to show that  $x_\gamma$  can be extended into a semi-norm on  $H_1(\Sigma, \partial\Sigma; \mathbb{R})$ .

## 2.2 Intersection norms

The main goal of this section is to extend the concept of intersection numbers defined over  $H_1(\Sigma, \partial\Sigma; \mathbb{Z})$  to a semi-norm defined over  $H_1(\Sigma, \partial\Sigma; \mathbb{R})$ . We extend  $x_\gamma$  on  $H_1(\Sigma, \partial\Sigma; \mathbb{R})$ .

### 2.2.1 Extension over $H_1(\Sigma, \partial\Sigma; \mathbb{R})$

**Definition 19.** *We define the semi-norm  $x_\gamma$  on  $H_1(\Sigma, \partial\Sigma; \mathbb{Q})$  by*

$$\forall q \in \mathbb{Q}, \forall a \in H_1(\Sigma, \partial\Sigma; \mathbb{Q}), x_\gamma(q.a) = q.x_\gamma(a)$$

The linearity on the rays (Lemma 15) assures that this extension is well-defined. The triangular inequality (Lemma 16) will allow us to extend this definition over  $H_1(\Sigma, \partial\Sigma; \mathbb{R})$ .

**Proposition 20.** *Let  $\Sigma$  be a compact oriented surface and  $\gamma$  a multi-curve on  $\Sigma$ . The function  $x_\gamma$  extends canonically into a continuous function  $x_\gamma : H_1(\Sigma, \partial\Sigma; \mathbb{R}) \rightarrow \mathbb{R}_+$  which is convex and linear on rays through the origin. If, furthermore, the multi-curve  $\gamma$  fills  $\Sigma$  in the sense that the complement  $\Sigma \setminus \gamma$  is the union of topological discs, then  $x_\gamma$  is a norm.*

*Proof.* The vector space  $H_1(\Sigma, \partial\Sigma; \mathbb{Q})$  is finite dimensional. We will note  $n$  its dimension. By the equivalency of norms on finite dimensional vector spaces, we just have to show the continuity of  $x_\gamma$  from  $(H_1(\Sigma, \partial\Sigma; \mathbb{Q}), \|\cdot\|_\infty)$  to  $\mathbb{R}$  endowed with its Euclidean metric. Consider  $x \in H_1(\Sigma, \partial\Sigma; \mathbb{Q})$ ,  $\|x\|_\infty \in \mathbb{Q}$ , we then have,  $\frac{x_\gamma(x)}{\|x\|_\infty} = x_\gamma\left(\frac{x}{\|x\|_\infty}\right)$ . Consider  $\rho \in H_1(\Sigma, \partial\Sigma; \mathbb{Q})$  such that  $\|\rho\|_\infty = 1$ ,  $\rho$  belongs to the unit ball of  $\|\cdot\|_\infty$  which is simply a  $n$ -hypercube. Let denote by  $(e_i)_{i \in 1 \dots 2^n}$  the vertices of this hypercube. We then have  $\rho = \sum_{i=1}^{2^n} a_i e_i$  with  $\sum_i a_i = 1$ ,  $a_i \geq 0$ . By sub-additivity (Lemma 15) we get  $x_\gamma(\rho) \leq \max_i (x_\gamma(e_i))$ . Let denote  $\delta_\gamma$  this real. Hence for all  $x \in H_1(\Sigma, \partial\Sigma; \mathbb{Q})$  we have  $x_\gamma(x) \leq \delta_\gamma \|x\|_\infty$ .  $x_\gamma$  is then Lipschitz continuous, hence continuous and can therefore be continuously extended to  $H_1(\Sigma, \partial\Sigma; \mathbb{R})$  by the density of  $H_1(\Sigma, \partial\Sigma; \mathbb{Q})$  into  $H_1(\Sigma, \partial\Sigma; \mathbb{R})$ .

The extension of  $x_\gamma$  is the norm if for every non-null homotopy class, the intersection number is null. Consider  $\alpha$  a minimizing closed multi-curve for a non-null homotopy class  $a$  in  $H_1(\Sigma, \partial\Sigma; \mathbb{Z})$ , since  $\Sigma/\gamma$  decomposes into a union of topological discs,  $\alpha$  crosses  $\gamma$  at least once since it is non-null homotopic.  $\square$

### 2.3 Intersection norms and Eulerian coorientations

A natural question is whether the vertices of  $B_\gamma^*$  (or equivalently the faces of  $B_\gamma$ ) have a nice interpretation. Pierre Dehornoy gave such an interpretation in [Deh16] in terms of Eulerian coorientations (Theorem 21). This gives a combinatorial interpretation of the dual unit ball of an intersection norm which is convenient for algorithmic applications.

Considering the multi-curve  $\gamma$  as a graph whose vertices are the double-points and whose edges are the simple arcs of  $\gamma$ , a *coorientation* of  $\gamma$  is the a choice of a coorientation for every edge of  $\gamma$ . A given multi-curve has only finitely many coorientations. A coorientation is *Eulerian* if around every double point, there are two positively and two negatively cooriented edges. A coorientation  $\nu$  can be algebraically paired with an oriented curve  $\alpha$  using signed intersection. If  $\nu$  is Eulerian, it turns out that the pairing  $\nu(\alpha)$  depends only on the homology class of  $\alpha$ , so that a Eulerian coorientation  $\nu$  induces an integral cohomology class  $[\nu] \in H^1(\Sigma; \mathbb{Z})$ . One can wonder which classes are represented by such Eulerian coorientations. A first remark is that representing a class  $a$  by a curve  $\alpha$  which minimizes the geometric intersection with  $\gamma$ , one sees that  $|\nu(a)|$  is not larger than  $x_\gamma(a)$ . A second remark is that the parity of  $\nu(a)$  is fixed by  $\gamma$ : indeed, since all intersection points are counted with a coefficient  $\pm 1$ , the parity of  $\nu(a)$  is determined by the parity of  $i_\gamma(\alpha)$  and does not depend on  $\nu$ ; since  $\gamma$  is a graph of even degree, the parity of  $i_\gamma(\alpha)$  does not change if we replace  $\alpha$  by a homologous curve. Our second result states that these restrictions are the only ones: the classes of the Eulerian coorientations are exactly the integer points in  $B_\gamma^*$  that are *congruent to  $[\gamma]_2 \pmod 2$* . More interestingly, the extremal points of  $B_\gamma^*$  correspond to some Eulerian coorientations.

**Theorem 21.** *Let  $\Sigma$  be a compact oriented surface and  $\gamma$  a multi-curve on  $\Sigma$ . The dual unit ball  $B_\gamma^*$  in  $H^1(\Sigma; \mathbb{R})$  is the convex hull of the points in  $H^1(\Sigma; \mathbb{Z})$  given by all Eulerian coorientations of  $\gamma$ . Equivalently, for every  $a$  in  $H_1(\Sigma, \partial\Sigma; \mathbb{Z})$ , we have*

$$x_\gamma(a) = \min_{[\alpha]=a} i_\gamma(\alpha) = \max_{\substack{\nu \text{ Eulerian} \\ \text{coor. of } \gamma}} \nu(a).$$

Moreover every point in  $B_\gamma^* \cap H^1(\Sigma; \mathbb{Z})$  that is congruent to  $[\gamma]_2 \pmod 2$  is the class of some Eulerian coorientation.

*Proof.* Proof in [Deh16] □

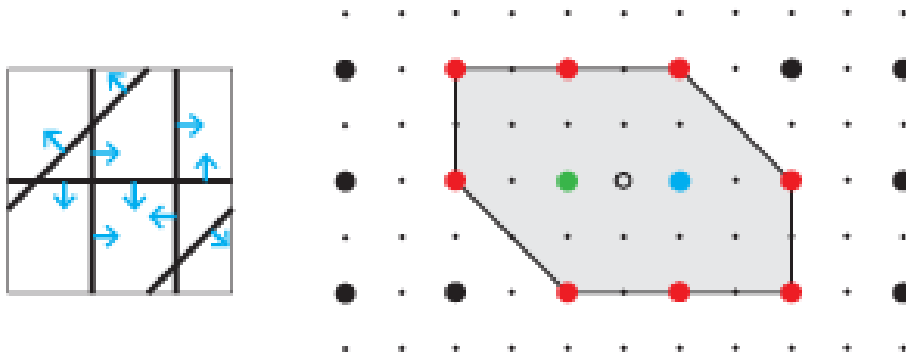


Figure 2: Illustration of Theorems 21. On the left a collection  $\gamma$  of four geodesics on the torus  $\mathbb{T}^2$ , and a Eulerian coorientation (blue arrows). On the right the dual unit ball  $B_\gamma^* \subset H_1(\mathbb{T}^2; \mathbb{Z})$  of the associated intersection norm. The empty circle denotes the origin. The big dots denote those classes in  $H_1(\mathbb{T}^2; \mathbb{Z})$  congruent to  $[\gamma]_2 \pmod 2$ .

**Remark 22.** *From an algorithmic point of view, this theorem gives a combinatorial way to compute the dual unit ball of an intersection norm if we know the curve that induces it. However, since the problem of counting Eulerian paths is  $\sharp\mathcal{P}$ -complete [Bri04], the approach consisting in generating all possible Eulerian orientations is not in  $\mathcal{P}$  under the assumption  $\mathcal{P} \neq \mathcal{NP}$ . Indeed, if it was, the BEST Theorem [Aar51] would provide a polynomial time algorithm to resolve the counting problem and  $\mathcal{P}$  would be equal to  $\mathcal{NP}$ .*

### 3 Intersection norms on the flat torus

#### 3.1 Normal polygons and Minkowski sum

The aim of this section is to present a simple decomposition of every normal polygon as a Minkowski sum (Theorem 30). A normal polygon is a convex polygon symmetric about the origin. Simple examples of such polygon are dual unitary ball of any intersection norm where  $H_1(\Sigma, \partial\Sigma; \mathbb{Z})$  is a  $\mathbb{Z}$ -module of rank two.

##### 3.1.1 Definitions

**Definition 23** (Normal polygon). *A convex polygon in  $\mathbb{R}^2$  is called normal if it is symmetric with respect to the origin.*

**Definition 24** (Minkowski sum). *Let  $E$  be a vector space, consider  $A$  and  $B$  two subsets of  $E$ . The Minkowski sum  $A \oplus B$  is defined as*

$$A \oplus B = \{x + y \mid x \in A, y \in B\}$$

**Definition 25.** *Given a finite family of non-null and non-pairwise collinear vectors  $\{\gamma_i\}_{i \in \llbracket 1;n \rrbracket}$  such that  $\sum_{i=1}^n \gamma_i = 0$  there exists one and only one convex polygon up to translation denoted  $P\left(\left\{\{\gamma_i\}_{i \in \llbracket 1;n \rrbracket}\right\}\right)$  such that the faces of  $P\left(\left\{\{\gamma_i\}_{i \in \llbracket 1;n \rrbracket}\right\}\right)$  are of the form  $\{x_0 + \lambda\gamma_i \mid \lambda \in [0; 1], x_0 \in \mathbb{R}^2\}$ .*

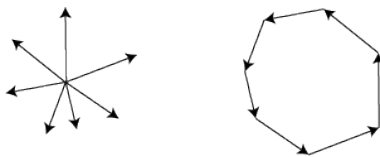


Figure 3: Illustration of Definition 25: On the right we see the convex polygon composed of the family of vectors on the left

**Definition 26.** *Consider  $\Gamma$  a polygon in  $\mathbb{R}^2$  and  $\sigma$  a face of  $\Gamma$ . We call support vectors of  $\sigma$  a vector  $\vec{\sigma}$  such that  $\sigma = \{x_0 + \lambda\vec{\sigma} \mid \lambda \in [0; 1], x_0 \in \mathbb{R}^2\}$  (a face admits exactly two support vectors which are opposite). Given a face  $\sigma$  we associate the centered face of  $\sigma$  denoted defined by*

$$\check{\sigma} = \left\{ \lambda \vec{\sigma} \mid \lambda \in \left[ -\frac{1}{2}; \frac{1}{2} \right] \right\}$$

The centered face  $\check{\sigma}$  does not depend on the choice of  $\vec{\sigma}$ .

**Remark 27.** If  $\Gamma$  is a normal polygon, then two opposite faces correspond to the same centered face. In fact the set of (non-redundant) centered faces characterize a normal polygon.

**Notation 1.** Given  $\Gamma$  a normal polygon, we will denote by  $\mathfrak{F}_\Gamma$  the set of non-redundant centered face of  $\Gamma$ .

**Definition 28** (Contraction of centered face). Let  $\Gamma$  be a normal polygon, given a centered face  $\sigma \in \mathfrak{F}_\Gamma$ , we define the contraction  $\mathfrak{C}_\Gamma(\sigma)$  of  $\sigma$  over  $\Gamma$  by

$$\mathfrak{C}_\Gamma(\sigma) = \left\{ x - \frac{1}{2}\vec{\sigma} \mid x \in \Gamma, \langle x \mid \vec{\sigma} \rangle \geq \frac{1}{2} \right\} \cup \left\{ x + \frac{1}{2}\vec{\sigma} \mid x \in \Gamma, \langle x \mid \vec{\sigma} \rangle \leq -\frac{1}{2} \right\}$$

This operation does not depend on the choice of  $\vec{\sigma}$ .

This operation simply corresponds to the contraction of the red band in Figure 4:  $\{x \in \Gamma \mid |\langle x \mid \vec{\sigma} \rangle| \in [-\frac{1}{2}; \frac{1}{2}]\}$ . The result of this operation,  $\mathfrak{C}_\Gamma(\sigma)$  corresponds to the normal polygon supported by  $\mathfrak{F}_\Gamma \setminus \{\sigma\}$ .

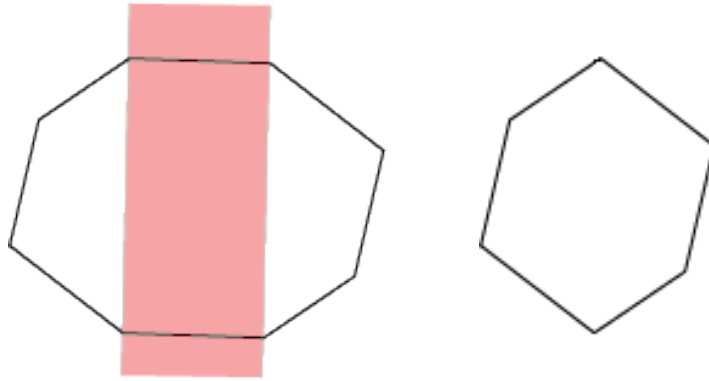


Figure 4: Illustration of the contraction of the face that supports the transparent red band of the normal polygon. From left to right, one can see the polygon before and after the contraction

**Notation 2.** Given  $\Gamma$  a normal polygon, given a centered face  $\sigma \in \mathfrak{F}_\Gamma(\sigma)$ , given  $\vec{\sigma}$  a support vector of  $\sigma$ , we denote by  $\Gamma_U$  the set

$$\Gamma_U = \left\{ x - \frac{1}{2}\vec{\sigma} \mid x \in \Gamma, \langle x \mid \vec{\sigma} \rangle \geq \frac{1}{2} \right\}$$

and by  $\Gamma_D$  the set

$$\Gamma_D = \left\{ x + \frac{1}{2}\vec{\sigma} \mid x \in \Gamma, \langle x \mid \vec{\sigma} \rangle \leq -\frac{1}{2} \right\}$$

We hereby have  $\mathfrak{C}_\Gamma(\sigma) = \Gamma_U \cup \Gamma_D$ . The choice of the opposite support vector exchanges the sets  $\Gamma_U$  and  $\Gamma_D$ .

**Lemma 29.** Let  $\Gamma$  be a normal polygon, let  $\sigma \in \mathfrak{F}_\Gamma$  be a centered face of  $\Gamma$ , then we have

$$\Gamma = \mathfrak{C}_\Gamma(\sigma) \oplus \sigma$$

*Proof.* We fix a support vector  $\vec{\sigma}$ . This choice will not influence the demonstration because we work with symmetrical sets and it will just exchange  $\Gamma_U$  and  $\Gamma_D$

- Consider  $x \in \Gamma$  and write  $x = \alpha\bar{\sigma} + \beta\bar{\delta}$  where  $\bar{\sigma}$  is the normalization of  $\vec{\sigma}$  and  $\bar{\delta} = \text{rot}_{\frac{\pi}{2}}(\bar{\sigma})$

- If  $|\langle x | \vec{\sigma} \rangle| < \frac{1}{2}$ , then  $\alpha$  belongs to  $\left] -\frac{\|\vec{\sigma}\|}{2}; \frac{\|\vec{\sigma}\|}{2} \right[$ . Without loss of generality, we will consider that  $\alpha \geq 0$ . Hence we have  $\left\langle x + \left( \frac{\|\vec{\sigma}\|}{2} - \alpha \right) \vec{\sigma} \mid \vec{\sigma} \right\rangle = \frac{1}{2}$  which gives  $x + \left( \frac{\|\vec{\sigma}\|}{2} - \alpha \right) \vec{\sigma} \in \Gamma_U$ . This gives the following decomposition:
- $$x = \underbrace{x + \left( \frac{\|\vec{\sigma}\|}{2} - \alpha \right) \vec{\sigma}}_{\substack{\in \Gamma_U \\ \in \mathfrak{C}_\Gamma(\sigma)}} - \frac{1}{2} \vec{\sigma} + \underbrace{\left( \frac{1}{2} + \alpha - \frac{\|\vec{\sigma}\|}{2} \right) \vec{\sigma}}_{\substack{\in [-\frac{1}{2}; \frac{1}{2}] \\ \in \sigma}}$$
- If  $x \in \Gamma_U$  then  $x = \underbrace{x - \frac{1}{2} \vec{\sigma}}_{\in \mathfrak{C}_\Gamma(\sigma)} + \underbrace{\frac{1}{2} \vec{\sigma}}_{\in \sigma}$ .
- The case  $x \in \Gamma_D$  is treated similarly.

Hence we have  $\Gamma \subseteq \mathfrak{C}_\Gamma(\sigma) \oplus \sigma$ .

- Consider  $x \in \mathfrak{C}_\Gamma(\sigma) \oplus \sigma$  and write  $x = x_1 + x_2$  with  $x_1 \in \mathfrak{C}_\Gamma(\sigma)$ ,  $x_2 \in \sigma$ . Without loss of generality, we can assume  $x_1 = a - \frac{1}{2} \vec{\sigma}$  with  $a \in \Gamma_U$ ,  $x_2 = \lambda \vec{\sigma}$  where  $\lambda \in [-\frac{1}{2}; \frac{1}{2}]$ . Since  $\langle x | \vec{\sigma} \rangle = \langle a - \frac{1}{2} \vec{\sigma} + \lambda \vec{\sigma} | \vec{\sigma} \rangle$ , we have

$$-\frac{1}{2} \leq \langle x | \vec{\sigma} \rangle = \left\langle a + \left( \lambda - \frac{1}{2} \right) \vec{\sigma} \mid \vec{\sigma} \right\rangle \leq \langle a | \vec{\sigma} \rangle$$

Since  $\langle x | \text{rot}_{\frac{\pi}{2}}(\vec{\sigma}) \rangle = \langle a | \text{rot}_{\frac{\pi}{2}}(\vec{\sigma}) \rangle$  we deduce that  $x$  belongs to  $\Gamma$ .

This leads to  $\Gamma \subseteq \mathfrak{C}_\Gamma(\sigma) \oplus \sigma$  which achieve the demonstration.  $\square$

We immediately obtain

**Theorem 30** (Decomposition of normal polygon). *Let  $\Gamma$  be a normal polygon,  $\Gamma$  decomposes into the Minkowski sum of its centered faces, i.e.*

$$\Gamma = \bigoplus_{\sigma_i \in \mathfrak{S}_\Gamma} \sigma_i$$

### 3.2 Case of geodesics on the flat torus

Geodesics form a particular class of curves on a Riemannian surface that are the "straightest" curves on the surface. In this section, we explore the properties of intersection norms when the closed multi-curve  $\gamma$  is made of a collection of geodesics on the torus. We will prove the main theorem of this Master's thesis which says that the geodesics are full for intersection norms in the sense that for every closed multi-curve  $\gamma$ , there exists a collection of geodesics such that the intersection norm induced by  $\gamma$  and the geodesic collection are the same. We will even give a simple way to express this collection using the dual unit ball of  $\mu_\gamma$ .

#### 3.2.1 Geodesics and minimality

In this section we show that if we consider the intersection norm for a union of geodesics, then geodesics are minimizing for any homology class in  $H_1(\mathbb{T}^2; \mathbb{Z})$ . We will first prove the case of intersection norms of a unique geodesic  $\gamma$ .

**Proposition 31** (Weak Geodesic Minimality Theorem). *For any  $a$  in  $H_1(\mathbb{T}^2; \mathbb{Z})$ , for any geodesic  $\alpha$  in the homology class  $a$  and for any geodesic  $\gamma$ , we have*

$$\mu_\gamma(a) = i_\gamma(\alpha)$$

*Proof.* Since  $\gamma$  is a geodesic, it is represented by a straight line in the universal covering  $\mathbb{R}^2$  of  $\mathbb{T}^2$ . Hence, there exists a transformation of  $\mathbb{T}^2$  in  $SL_2(\mathbb{R})$  such that its action on  $\mathbb{R}^2$  brings the representation of  $\gamma$  on the abscissa. In this case, for any homotopy class  $a$ , the intersection number is the minimum of number of time a curve in  $a$  crosses the abscissa which can be achieved by a geodesic.  $\square$

From this we immediately deduce a stronger theorem which applies to a finite collection of geodesics.

**Theorem 32** (Geodesic Minimality Theorem). *For any  $a$  in  $H_1(\mathbb{T}^2; \mathbb{Z})$ , for any geodesic  $\alpha$  in the homology class  $a$ , and for any collection of geodesics  $\gamma_1, \dots, \gamma_n$  we have*

$$\mu_{\gamma_1 \cup \dots \cup \gamma_n}(a) = i_{\gamma_1 \cup \dots \cup \gamma_n}(\alpha)$$

*Proof.* For every geodesic  $\gamma_j$ , the minimal intersection number  $i_{\gamma_j}(a)$  is accomplished by  $\alpha$ . Hence  $\alpha$  minimizes all intersection number for all the geodesic and hence minimizes the intersection number of the whole collection which proves the theorem.  $\square$

This theorem is important because it allows to decompose the dual unitary ball of the intersection norm of a collection of geodesic into the Minkowski sum of all the unitary ball of every geodesic in the collection. This theorem implies indeed the additivity of the intersection norms for geodesic which combined with Proposition 8 brings us the decomposition.

### 3.2.2 Intersection norms of family of geodesic

**Theorem 33** (Additivity of intersection norms of geodesics). *Let  $\gamma_1, \dots, \gamma_n$  be a finite collection of geodesics over the flat torus, then we have*

$$\mu_{\gamma_1 \cup \dots \cup \gamma_n} = \sum_{i=1}^n \mu_{\gamma_i}$$

*Proof.* Consider  $a$  in  $H_1(\mathbb{T}^2; \mathbb{Z})$  and  $\alpha$  a geodesic in the homology class  $a$ . Using Theorem 32 we get  $\mu_{\gamma_1 \cup \dots \cup \gamma_n}(a) = i_{\gamma_1 \cup \dots \cup \gamma_n}(\alpha) = \sum_{i=1}^n i_{\gamma_i}(\alpha)$  since for every  $\gamma_i$  we have  $i_{\gamma_i}(\alpha) = \mu_{\gamma_i}(\alpha)$  (Proposition 31), we obtain  $\mu_{\gamma_1 \cup \dots \cup \gamma_n} = \sum_{i=1}^n \mu_{\gamma_i}$ .  $\square$

As we said previously using Proposition 8 we immediately get

**Corollary 34** (Geodesic dual decomposition theorem). *Let  $\gamma_1, \dots, \gamma_n$  be a finite collection of geodesics over the flat torus, then we have*

$$B_{\gamma_1 \cup \dots \cup \gamma_n}^* = \bigoplus_{i=1}^n B_{\gamma_i}^*$$



### 3.2.3 Intersection norm and dual unitary ball of the intersection norm of a geodesic

**Notation** For any homology class  $a$  in  $H_1(\mathbb{T}^2; \mathbb{Z})$ , we denote by  $\tilde{a}$  the segment  $[-a, a]$  in  $H_1(\mathbb{T}^2; \mathbb{Z})$ .

**Proposition 35.** *Consider  $\gamma$  a geodesic on  $\mathbb{T}^2$ , then we have  $B_\gamma^* = [\tilde{\gamma}]$ .*

*Proof.* This is a simple application of Theorem 21 by considering the curve as a graph with one vertex and one edge.  $\square$

This immediately gives

**Corollary 36.** *Consider  $\gamma$  a geodesic on  $\mathbb{T}^2$ . For every homology class  $a$  in  $H_1(\mathbb{T}^2; \mathbb{Z})$  we have  $x_\gamma(a) = |\det(a, [\gamma])|$*

### 3.2.4 Fulness theorem on the torus

This section proves two important theorems on intersection norms on the torus.

**Notation 3.** *For any centered segment  $\sigma = [-a, a]$ ,  $a \neq 0$  in  $H_1(\mathbb{T}^2; \mathbb{Z})$ , we denote by  $\sigma^*$  the homology class  $a$  such that  $\arg(a)$  is minimal (the argument precision is only here to ensure that this operation is well defined).*

**Theorem 37.** *For any closed multi-curve  $\gamma$  on  $\mathbb{T}^2$ , there exists a finite collection of geodesics  $\gamma_1, \dots, \gamma_n$  on  $\mathbb{T}^2$  such that  $\mu_\gamma = \mu_{\gamma_1 \cup \dots \cup \gamma_n}$ . Moreover one collection is given by a collection of geodesic with  $\left\{ \sigma^* \in H_1(\mathbb{T}^2; \mathbb{Z}) \mid \sigma \in \mathfrak{F}_{B_\gamma^*} \right\}$  as homology classes. In the case where one  $\sigma^*$  has its coordinates not coprime, we denote by  $n$  the greatest common divider of those coordinates and we consider  $n$  parallel copies of a geodesic with  $\sigma^*/n$  as homology class. Such decomposition is unique up to translations of the geodesics and reversing orientations of those.*

*Proof.* Consider the normal polygon  $B_\gamma^*$ , for every centered face  $\sigma$  in  $\mathfrak{F}_{B_\gamma^*}$ ,  $\sigma$  is of the form  $[-a, a]$  with  $a$  being a homology class with integral coefficients. This comes from Theorem 21 which ensures that the extremities of one face have the same parity. Indeed, this implies that when centered, the vertices of the face keep integral coefficients. Hence the centered faces are the dual unit ball of geodesics in homology class  $\sigma^*$ . The recomposition of  $B_\gamma^*$  is assured by Corollary 34.  $\square$

Associated with Corollary 36 we immediately get

**Corollary 38** (Explicit formula for intersection norms on the torus). *For any closed multi-curve  $\gamma$  on  $\mathbb{T}^2$  we have*

$$\forall a \in H_1(\mathbb{T}^2; \mathbb{Z}), \mu_\gamma = \sum_{\sigma \in \mathfrak{F}_{B_\gamma^*}} \left| \det \left( a, \left[ \sigma^* \right] \right) \right|.$$

**Theorem 39.** *Any normal polygon with integral vertices of same parity is realizable by a family of geodesic. Moreover, those are the only polygons realizable as intersection norms of closed multi-curve on  $\mathbb{T}^2$ .*

*Proof.* This is a direct consequence of Corollary 34 along with the restriction of the parity of the vertices of the dual unit ball given by Theorem 21.  $\square$

**Remark 40.** *Most of the consideration used in the proof of theorems on the geodesic collections on the torus are no longer true in higher genus and hence the generalization of these theorems are not trivial.*

## 4 Software

### 4.1 Presentation

**Disclaimer:** All technical content written in this document represents the state of the software and the technology as it is on June the 10<sup>th</sup> 2016. The source code of the software is available at <https://github.com/PCottalorda/MT/>.

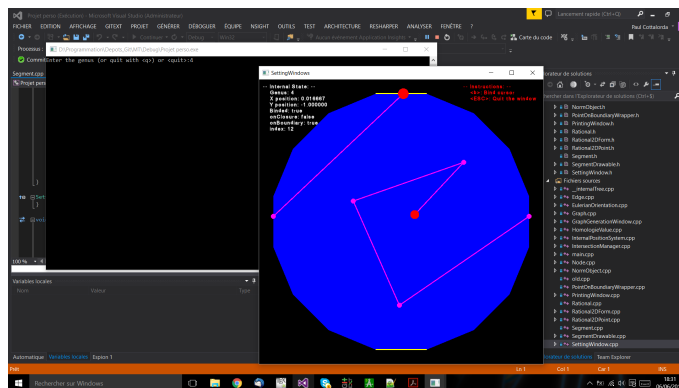


Figure 5: The software at runtime. One can see from the background to the foreground Microsoft Visual Studio, and the console user interface and the control window

The largest part of the internship consisted in developing a program allowing to compute examples of intersection norms. The development included different approaches and the development of different algorithms but the final version only kept the Eulerian approach allowed by Theorem 21. The project was developed under Microsoft Visual Studio Ultimate 2013 and hence has the structure of a Microsoft Visual Studio project but an adaptation to be cross-platform using a Makefile is expected. The source code and software are distributed under the Apache License Version 2.0 [Apache2.0]. The software depends on two external libraries Boost [Boost] and SFML [SFML] which are both cross-platform. The program compiles with any compiler supporting the C++14 standard and the preprocessor instruction `#pragma once`. This is the case for most of the main C++ compiler such as Clang [1], GCC [2], Microsoft Visual C++ Compiler [3], Intel C++ Compiler [4], IBM XL C/C++ [5], *etc.* with the main notable exception being Solaris Studio C/C++ [6].

#### 4.1.1 Limitations

- The software only works with orientable 2-manifolds without boundaries.
- The general complexity of the algorithm is exponential.
- No generic catcher at the highest level of the program.
- Possible overwrite of previous computed files (even it is VERY unlikely -(number of files already computed)/ $2^{32}$  on x86\_64 architectures-).

#### 4.1.2 Features

- A minimal User Interface in a console (Figure 6).

```

D:\Programmation\Depots_Git\MP\Debug\Projet perso.exe
Enter the genus (or quit with <q> or <quit>:3
Save image of the multi-lacet...
Done.
Compute Unitary Ball (this can take a while)...
Regroupement of all segments...
Done.
Computation of all intersections...
Done.
Regroupement of all the intersection points...
Done.
Create and fill the graph...
Done.
Generation of all the eulerian coorientation...
New eulerian orientation found [1]
New eulerian orientation found [2]
New eulerian orientation found [3]
New eulerian orientation found [4]
New eulerian orientation found [5]
New eulerian orientation found [6]
New eulerian orientation found [7]
New eulerian orientation found [8]
New eulerian orientation found [9]
New eulerian orientation found [10]
New eulerian orientation found [11]
New eulerian orientation found [12]
Done. (12 found).
Evaluation of all the eulerian coorientation found...
Done.
Done.
Enter the genus (or quit with <q> or <quit>:

```

Figure 6: Screenshot of the output of one execution of the program

- A control window allowing to enter and set the multi-curve from which we want to compute the intersection norm (Figure 7).

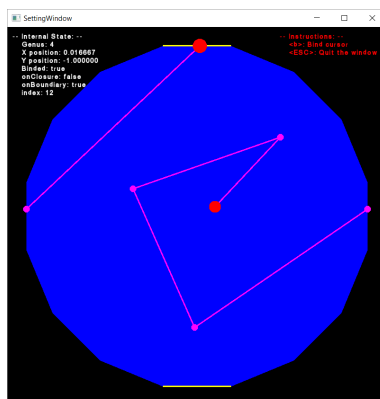
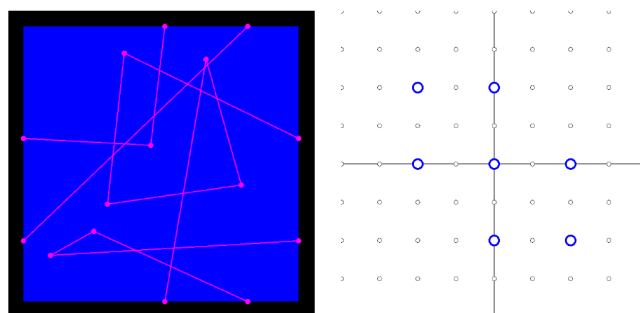


Figure 7: The control Window

- A  $\text{\LaTeX}$  generator joined with a picture generator that allows to generate  $\text{\LaTeX}$  files to save the norm computed. We can see on Figure 8 an example of the output of the software.



Eulerian points : [-2,0], [-2,2], [0,-2], [0,0], [0,2], [2,-2], [2,0]

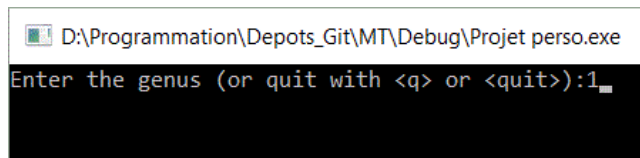
Figure 8:  $\text{\LaTeX}$  file generated by the software

## 4.2 Quick guide

This section is a guide on how to use the software.

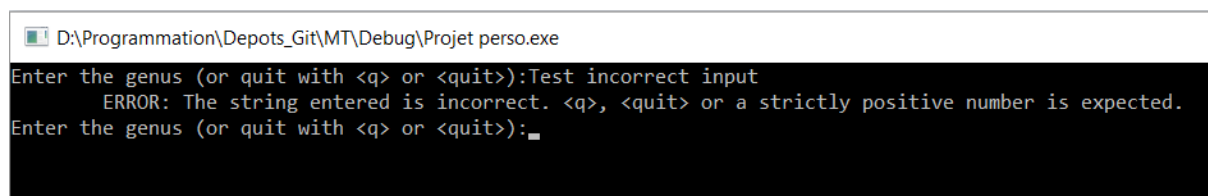
### 4.2.1 Choosing the genus

When one launch the program, a consol window open (if it hasn't been launched from a terminal) and a message is displayed on the standard output. The images from this guide has been made on the operating system Windows 10.



```
D:\Programmation\Depots_Git\MT\Debug\Projet perso.exe
Enter the genus (or quit with <q> or <quit>):1_
```

The program asks to enter the genus of the surface on which you will enter your closed multi-curves ("Enter the genus (or quit with <q> or <quit>):"). You can also choose to quit by typing `q` or `quit`. If you enter a negative or null number or if you type a non-numeric chain of character other than `q` or `quit`, then an error message is displayed and the program asks once again to enter the genus of the surface.



```
D:\Programmation\Depots_Git\MT\Debug\Projet perso.exe
Enter the genus (or quit with <q> or <quit>):Test incorrect input
ERROR: The string entered is incorrect. <q>, <quit> or a strictly positive number is expected.
Enter the genus (or quit with <q> or <quit>):_
```

### 4.2.2 Entering the closed multi-curves

Once one has entered a valid input for the genus, a new window is displayed (the Control Window). One can see different parts on this window. First of all, the big blue square corresponds to the fundamental polygon of the closed compact surface with the genus chosen on the previous step (here a torus (genus 1), but on Figure 7 one can see an example with a genus 4 surface).

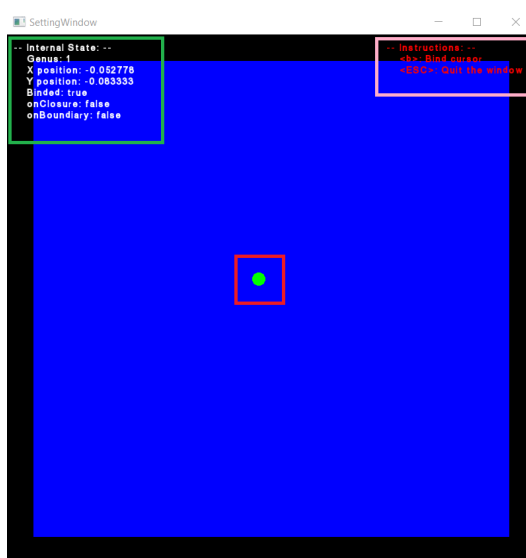


Figure 9: The program at runtime: Opening of the control window.

Four main pieces of information are displayed on the window:

1. The fundamental polygon here in blue.
2. The internal state of the program here framed in the green box on the top left of the screen. It provides:
  - The genus of the surface.
  - The position of the cursor within the fundamental polygon.
  - The state of the cursor (binded or not to the window), which means that the cursor is forced to stay on the fundamental polygon. This is the only state where you can enter a curve on the program.
  - Whether the cursor is on the first point of the current curve being entered (`onClosure`) or not.
  - Whether the cursor is on a boundary of the fundamental polygon or not (`onBoundary`). In the positive case, the index of the boundary is displayed.
3. An instruction part here framed in the pink box on the top right of the screen.
4. The cursor here framed in the red box on the center of the screen. On this picture, the cursor is displayed as a green ball. This is the way it is displayed when it is binded to the window and not on a boundary of the fundamental polygon. When the cursor is on a boundary of the fundamental polygon, the cursor is displayed in red (pink circle on Figure 11).

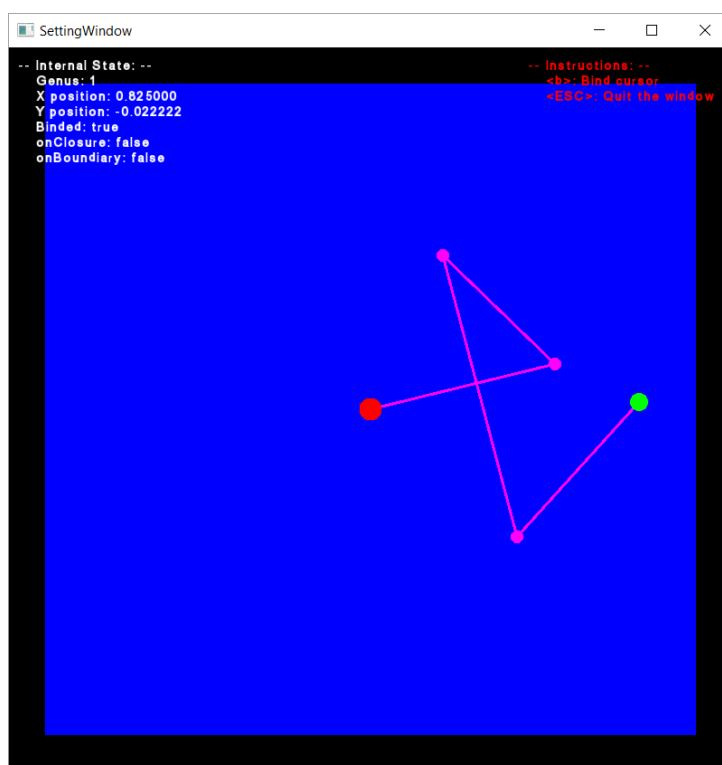


Figure 10: The program at runtime: Beginning to set the polylines.

Once the curve is binded one can click to place the points of the polyline that will be used to represent the closed multi-curves. The first point is always displayed in red (brown rhombus on Figure 11), and for every click the program sets a new point of the polyline. This first point can not be placed on a boundary.

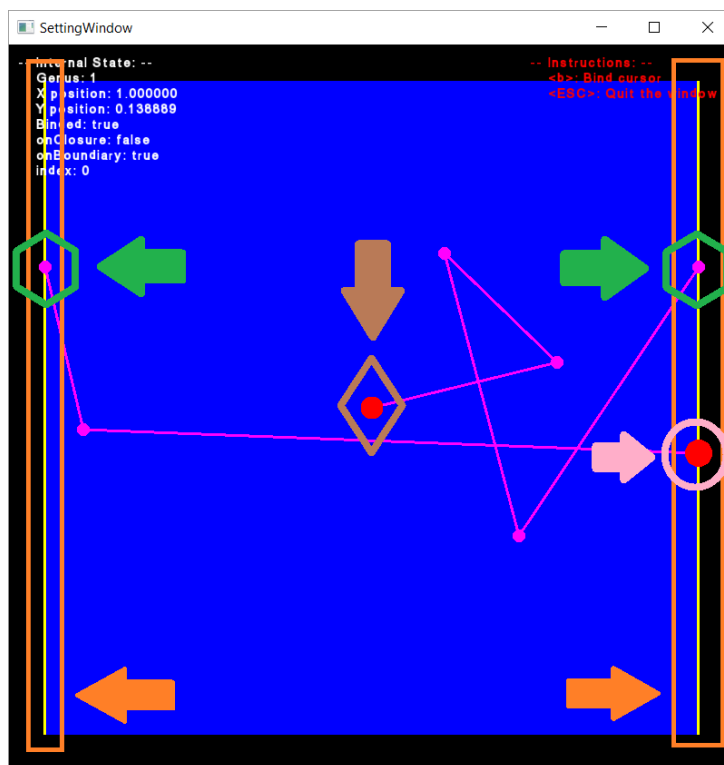


Figure 11: The program at runtime, with the cursor on the boundary.

When a point is fixed to the boundary, the corresponding boundary is displayed in yellow (orange squares on Figure 11), the boundaries attract the cursor if it is near which is more comfortable to the user. When a point is fixed on the boundary, the cursor is immediately transported at the opposite border which is topologically the same (green hexagon on Figure 11). When the user wants to close one curve he only has to put the cursor on the initial point of the curve. The initial point as well as the boundaries attracts the cursor in order to facilitate the closing process.

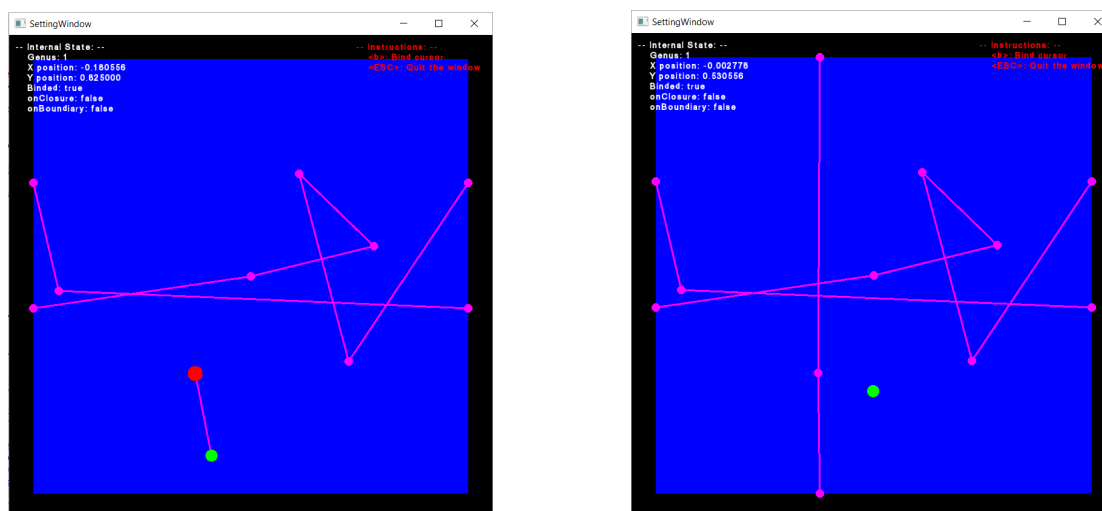


Figure 12: The program at runtime: Setting of multiple curves.

Once a polyline has been set, the user can enter another one using the same process as for the first one (Figure 12). Once the user has finished setting all the polyline representing

the desired closed multi-curve, he can press `<ESC>` to compute the associated intersection norm. Once the escape key has been pressed, the norm is computed (output on Figure 14), the window is closed and a  $\text{L}^{\text{A}}\text{T}_{\text{E}}\text{X}$  file is generated on the `GenData` folder (which needs to be created first). In this example, the program was generated in under 2 second in `Debug` compilation option.

```

D:\Programmation\Depots_Git\MT\Debug\Projet perso.exe
Enter the genus (or quit with <q> or <quit>):Test incorrect input
ERROR: The string entered is incorrect. <q>, <quit> or a strictly positive number is expected.
Enter the genus (or quit with <q> or <quit>):1
Save image of the multi-lacet...
Done.
Compute Unitary Ball (this can take a while)...
Regroupment of all segments...
Done.
Computation of all intersections...
Done.
Regroupment of all the intersection points...
Done.
Create and fill the graph...
Done.
Generation of all the eulerian coorientations...
New eulerian orientation found [1]
New eulerian orientation found [2]
New eulerian orientation found [3]

New eulerian orientation found [46]
New eulerian orientation found [47]
New eulerian orientation found [48]
New eulerian orientation found [49]
New eulerian orientation found [50]
New eulerian orientation found [51]
New eulerian orientation found [52]
New eulerian orientation found [53]
New eulerian orientation found [54]
New eulerian orientation found [55]
New eulerian orientation found [56]
Done. (56 found).
Evaluation of all the eulerian coorientation found...
Done.
Done.
Enter the genus (or quit with <q> or <quit>):_

```

Figure 13: The program at runtime: Output of the program.

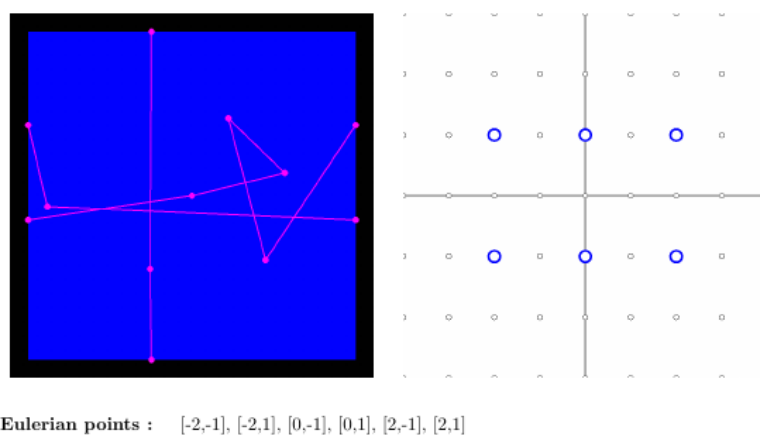


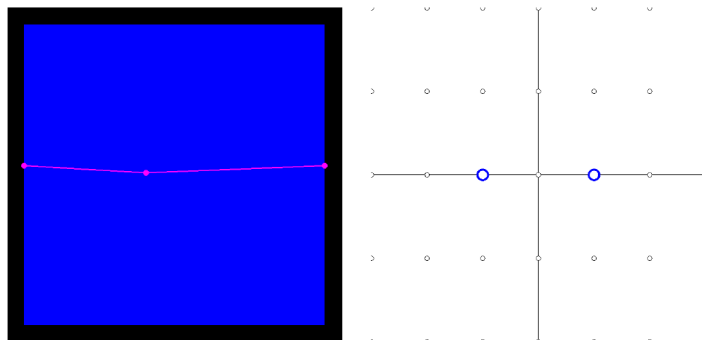
Figure 14: File generated by the program.

### 4.3 Performances

This section introduces four quick examples with their computation time. The tests has been realized on an Intel Core i7 5500U 2.4GHz and 16Go of RAM. The computation times given are internal.

#### Example 41.

- *Output:*

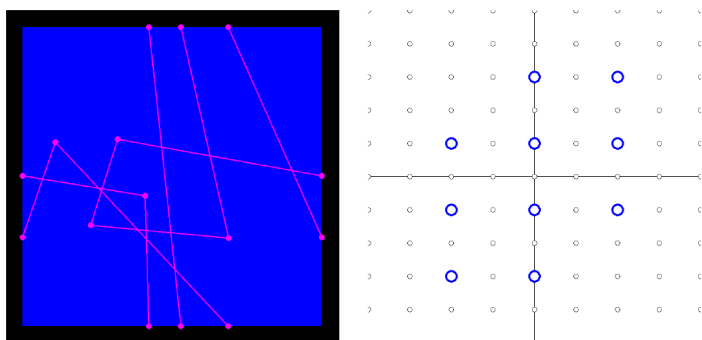


Eulerian points :  $[-1,0], [1,0]$

- *Number of points: 2*
- *Number of Eulerian orientations: 2*
- *Computation time: 17ms*

#### Example 42.

- *Output:*



Eulerian points :  $[-2,-3], [-2,-1], [-2,1], [0,-3], [0,-1], [0,1], [0,3], [2,-1], [2,1], [2,3]$

- *Number of points: 22*
- *Number of Eulerian orientations: 834*
- *Computation time: 6410ms*





- *Number of Eulerian orientations: 2750*
- *Computation time: 42277ms (42s).*

#### 4.4 Possible improvement

- The main battle neck of the program is the generation of Eulerian orientations. In order to have a working version as soon as possible, I made a non-optimal version of the orientations generator. A faster version using pre-computed material can greatly increase the computing speed.
- Support of the boundaries.
- Documentation for the program.
- A file management system.
- A generator of a C++ functor (eventually serialized) of the intersection norm using formula of Corollary 38.
- A parallelized version of the program.

## References

- [Sal16] DE LA SALLE Mikael: Another proof of Thurston’s theorem for norms taking integer values on the integer lattice, arXiv:1604.01578
- [Thu86] THURSTON William: A norm for the homology of three-manifolds, *Mem. Amer. Math. Soc.* **339** (1986), 99–130.
- [Bri04] BRIGHTWELL Graham R.: Note on Counting Eulerian Circuits, arXiv:cs/0405067
- [Deh16] DEHORNOY Pierre: Intersection norms on surfaces and Birkhoff surfaces for geodesic flows, arXiv:1604.06688
- [Aar51] VAN AARDENNE-EHRENFEST Tatiana Pavlovna and DE BRUIJN Nicolaas Govert: Circuits and trees in oriented linear graphs, *Simon Stevin* **28** (1986), 203–217.
- [Apache2.0] Apache License Version 2.0, <http://www.apache.org/licenses/LICENSE-2.0>
- [Boost] Boost C++ library, <http://www.boost.org>
- [SFML] Simple and Fast Multimedia Library, <http://www.sfml-dev.org>
- [1] Clang: Pragma.cpp Source File, [http://clang.llvm.org/doxygen/Pragma\\_8cpp-source.html#1](http://clang.llvm.org/doxygen/Pragma_8cpp-source.html#1)
- [2] GCC: GCC 3.4 Release Series — Changes, New Features, and Fixes, <https://gcc.gnu.org/gcc-3.4/changes.html>
- [3] MSDN: once C/C++, [https://msdn.microsoft.com/en-us/library/4141z1cx\(v=vs.71\).aspx](https://msdn.microsoft.com/en-us/library/4141z1cx(v=vs.71).aspx)
- [4] Intel: Diagnostic 1782: #pragma once is obsolete. Use #ifndef guard instead, <https://software.intel.com/en-us/articles/cdiag1782#comment-9466>
- [5] IBM: Supported GCC pragmas, [http://www.ibm.com/support/knowledgecenter/SSXVZZ\\_13.1.com.ibm.xlcpp1311.linux.doc/compiler\\_ref/pragmas\\_gcc\\_clang\\_support.html](http://www.ibm.com/support/knowledgecenter/SSXVZZ_13.1.com.ibm.xlcpp1311.linux.doc/compiler_ref/pragmas_gcc_clang_support.html)
- [6] Solaris: Solaris Studio 12.4: C++ User’s Guide, [https://docs.oracle.com/cd/E37069\\_01/html/E37075/bkbcju.html](https://docs.oracle.com/cd/E37069_01/html/E37075/bkbcju.html)